New Journal of Physics
The open-access journal for physics

Encoding a qubit into multilevel subspaces

Matthew Grace[1], **Constantin Brif**[1], **Herschel Rabitz**[1,6], **Ian Walmsley**[2], **Robert Kosut**[3] **and Daniel Lidar**[4,5]

[1] Department of Chemistry, Princeton University, Princeton, NJ 08544, USA
[2] Department of Physics, University of Oxford, Oxford OX1 3PU, UK
[3] SC Solutions, Inc., 1261 Oakmead Parkway, Sunnyvale, CA 94085, USA
[4] Department of Chemistry, University of Toronto,
Toronto ON M5S 3H6, Canada
E-mail: mgrace@princeton.edu, cbrif@princeton.edu, hrabitz@princeton.edu, walmsley@physics.ox.ac.uk, kosut@scsolutions.com and lidar@usc.edu

New Journal of Physics **8** (2006) 35
Received 12 September 2005
Published 9 March 2006
Online at http://www.njp.org/
doi:10.1088/1367-2630/8/3/035

Abstract. We present a formalism for encoding the logical basis of a qubit into subspaces of multiple physical levels. The need for this multilevel encoding (MLE) arises naturally in situations where the speed of quantum operations exceeds the limits imposed by the addressability of individual energy levels of the qubit physical system. A basic feature of the MLE formalism is the logical equivalence of different physical states and correspondingly, of different physical transformations. This logical equivalence is a source of a significant flexibility in designing logical operations, while the multilevel structure inherently accommodates fast and intense broadband controls thereby facilitating faster quantum operations. Another important practical advantage of MLE is the ability to maintain full quantum-computational fidelity in the presence of mixing and decoherence within encoding subspaces. The formalism is developed in detail for single-qubit operations and generalized for multiple qubits. As an illustrative example, we perform a simulation of closed-loop optimal control of single-qubit operations for a model multilevel system, and subsequently apply these operations at finite temperatures to investigate the effect of decoherence on operational fidelity.

[5] Present address: Departments of Chemistry, Electrical Engineering-Systems and Physics, University of Southern California, Los Angeles, CA 90089, USA.
[6] Author to whom any correspondence should be addressed.

PII: S1367-2630(06)07904-3

Contents

1. Introduction

Quantum computation is an extremely active area of research, with potential realizations ranging from solid state to atomic and optical systems [1, 2]. Following seminal work on ideal quantum computation, the focus of research has shifted in recent years to practical issues of implementing scalable quantum gates in real systems in the presence of noise, decoherence and imperfect controls. One significant issue is the fundamental process of decoherence caused by coupling to the environment. Another obstacle is noise that, in any practical situation, exists in external control fields which are normally required to perform the logical operations of quantum information processing [3]. In order to ensure fault-tolerant operation of quantum registers, errors, including those associated with environmentally induced decoherence and control field noise, must be minimized below a specified threshold [4]. Since external controls are essential for logical operations, it is reasonable to assume that practical implementations of quantum computation, especially in relatively complex physical systems, can be greatly facilitated by the powerful methods of optimal control [5, 6]. Closed-loop adaptive laboratory control is of special importance because of its inherent robustness to noise and suitability for managing complex physical systems [5]–[12]. Furthermore, intense ultrafast control fields, which are essential for accelerating quantum operations, thereby diminishing the effect of decoherence, are especially suited for closed-loop laboratory control. Applying the methods of optimal control to various realizations of quantum computation was recently considered in a number of works [13]–[22].

The majority of schemes proposed for physical realizations of quantum computation assign a single physical level to represent each of the logical basis states ($|0\rangle$ and $|1\rangle$) of a qubit. In such a situation, each logical operation is represented by a unique physical transformation [1]. In this paper we consider a more general situation, where each logical basis state is encoded into a subspace of multiple physical levels. This generalization leads to the logical equivalence of different physical states, i.e., different multilevel superpositions can represent the same logical state of a qubit. Correspondingly, with multilevel encoding (MLE) there will exist different physical transformations which will also be logically equivalent, i.e., these transformations represent the same logical operation.

An important question is whether the use of MLE yields any practical advantages in comparison to the usual single-level encoding (SLE). The following analysis indicates that MLE is a natural choice when the need to accelerate quantum operations requires the bandwidth of control fields to exceed the separation between energy levels of a quantum register. For systems with a dense energy spectrum, the factor determining individual level addressability is the ratio between the bandwidth, $\Delta\Omega$, of the external control field and the characteristic energy-level spacing, $\Delta\omega$, of the physical system that realizes the register. In the limit of slow control, i.e., $\Delta\Omega < \Delta\omega$, logical basis states can be encoded into single physical levels and MLE is not necessary. While such slow controls may be satisfactory for proof-of-principle experiments, practical realizations of quantum registers in many cases will require much faster operations and correspondingly, faster controls, with $\Delta\Omega \gg \Delta\omega$. In such a case, one must take into account the various transitions between the multiple states driven by a control field. Encoding each logical basis state into a subspace of multiple physical levels circumvents this issue, since addressability of individual levels within each subspace is not necessary due to the principle of logical equivalence developed in this work.

It is clear from the arguments above that the importance of MLE depends on the specific physical realization of a quantum register, so it will be helpful to consider specific examples of systems which may be suitable for realizations of MLE. One such system is a molecule in which the logical basis of a qubit is realized by vibrational states on the ground and/or excited electronic surfaces [23, 24]. For example, typical vibrational periods in homonuclear alkaline dimers range from 300 to 500 fs [25]. If the system is driven by ultrafast laser pulses of durations ranging from 20 to 100 fs (which are currently successfully used in closed-loop adaptive control experiments with molecular systems [26]–[32]), many transitions between vibrational levels will be driven simultaneously. In such a case, it can be useful to encode each logical basis state into a set of multiple molecular levels.

Another interesting example is a system whose internal levels are used for the logical basis while it is spatially confined in an external potential (e.g., an ion in an electromagnetic trap or an atom in an optical lattice). In the majority of schemes proposed for quantum computation with trapped ions, the gate time is limited by the trap frequency, mainly due to the need to spectroscopically resolve the motional sidebands [33]–[37]. This is a serious limitation because typical ion-trap frequencies are relatively low, ranging from 100 kHz to 100 MHz [38, 39]. External controls which are faster than the vibrational frequency of a trapped qubit will inevitably excite multiple motional levels. This effect will be especially important outside of the Lamb–Dicke limit, i.e., when multiple sidebands are excited by a laser field interacting with a trapped ion. Encoding each logical basis state into multiple motional levels of a trapped particle can be a useful approach in situations when fast controls are desired.

An idea related to the concept of MLE was recently proposed by García-Ripoll *et al* [40], who considered a two-qubit operation acting on a pair of trapped ions. The essence of this proposal is to apply coherent laser controls which leave the initial motional state unchanged at the end of the sequence of control pulses, thereby allowing for operations which are much faster than the trap frequency. MLE allows for more general operations (not just the identity operation) on the motional levels which constitute the encoding subspaces for a trapped particle. However, MLE may not be directly applicable to popular schemes where the common motional mode of a number of trapped ions is additionally employed to entangle the internal atomic states of different qubits. At this point it is not yet clear which systems will be most suitable for MLE in practical realizations of quantum computation, but the importance of MLE will increase in line with the acceleration of quantum operations.

Searching for an optimal control field to perform a logical operation on a multilevel system can benefit from MLE due to the logical equivalence of different physical transformations. Also, the multiplicity of logically equivalent physical transformations can facilitate finding optimal operations with improved robustness against noise in external controls [41]. Moreover, multiple physical transformations which realize the same logical operation may be used interchangeably throughout the computation, providing greater flexibility in the laboratory implementation of controls.

Perhaps the most important property of MLE is its utility as a practical instrument to reduce the effects of mixing in the initial quantum state (e.g., due to thermal excitations) and decoherence throughout the computation. In many practical situations, the initialization of a quantum register requires cooling a system to the ground state since the impurity of the initial state due to thermal excitations reduces quantum-computational fidelity. This cooling is often a difficult and slow process, therefore a practical alternative is desirable. Another significant source of errors is decoherence during logical operations. A possible way to overcome these problems is, once again, by encoding the logical basis into subspaces of multiple physical levels. Due to the principle of logical equivalence, mixing and decoherence *within* each encoding subspace do not affect coherence *between* the two logical basis states and therefore do not reduce computational fidelity.

This paper is organized as follows. In section 2, the concept and mathematical formalism of MLE are developed for a single qubit. Logical equivalence resulting from MLE is defined for physical states and transformations, and equivalence classes of logical states and operations are introduced. In section 3, the MLE formalism and corresponding logical equivalence are used to construct single-qubit unitary operations and derive their general form (a tensor-product structure (TPS)). Section 4 extends the MLE formalism to mixed states and non-unitary operations. In particular, this allows for logical equivalence between pure and mixed states, and between unitary and general non-unitary (permitting decoherence) quantum operations, provided that full coherence exists between the encoding subspaces. In section 5, we demonstrate the formalism and some of its advantages by performing a numerical simulation of closed-loop optimal control of single-qubit operations for a model system based on the electronic and vibrational levels of an alkaline dimer, and applying the resulting operations at finite temperatures. In sections 6 and 7, the MLE formalism is generalized for logical states and operations of multiple qubits. As in the single-qubit case, a general tensor-product form for multi-qubit unitary operations is obtained. Section 8 concludes the paper with a brief summary of the results, open questions and future directions.

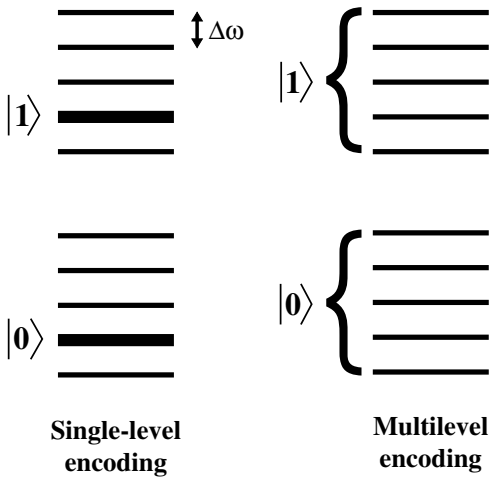

Figure 1. A sample scheme that illustrates the difference between SLE and MLE of logical basis states of a qubit.

2. Concept and formalism

For a single qubit, MLE involves partitioning the energy levels of a given quantum system into two distinct subspaces of equal dimension, the 'encoding subspaces' $\mathcal{S}_0$ and $\mathcal{S}_1$. Let $|\boldsymbol{a}\rangle$ denote *any* element of $\mathcal{S}_0$ such that $\langle \boldsymbol{a}|\boldsymbol{a}\rangle = 1$ and $|\boldsymbol{b}\rangle$ denote *any* element of $\mathcal{S}_1$ such that $\langle \boldsymbol{b}|\boldsymbol{b}\rangle = 1$, i.e.,

$$|\boldsymbol{a}\rangle = \sum_{i=1}^{n} a_i|\chi_i\rangle = (a_1 \cdots a_n)^T, \qquad \text{such that } \langle \boldsymbol{a}|\boldsymbol{a}\rangle = \sum_{i=1}^{n} |a_i|^2 = 1 \tag{1}$$

and

$$|\boldsymbol{b}\rangle = \sum_{i=1}^{n} b_i|\phi_i\rangle = (b_1 \cdots b_n)^T, \qquad \text{such that } \langle \boldsymbol{b}|\boldsymbol{b}\rangle = \sum_{i=1}^{n} |b_i|^2 = 1. \tag{2}$$

Here n is the dimension of the encoding subspaces and $\{|\chi_i\rangle\}$ and $\{|\phi_i\rangle\}$ are orthonormal bases that span $\mathcal{S}_0$ and $\mathcal{S}_1$, respectively. Correspondingly, $\langle \chi_i|\chi_j\rangle = \langle \phi_i|\phi_j\rangle = \delta_{ij}$ and $\langle \chi_i|\phi_j\rangle = 0$. It is important to emphasize that for each subspace ($\mathcal{S}_0$ or $\mathcal{S}_1$) there exists an infinite set of states that satisfy the respective criteria of (1) or (2). Within this framework each logical basis state is encoded into one of these subspaces (figure 1). Therefore, the Hilbert space of an encoded qubit (which is two-dimensional in the SLE representation) corresponds to an expanded (and higher dimensional) Hilbert space of physical levels. In this expanded Hilbert space the logical basis states are expressed as

$$|0\rangle = |0\rangle_{\mathrm{L}} \otimes |\boldsymbol{a}\rangle = \Big(a_1 \cdots a_n \underbrace{0 \cdots 0}_{n}\Big)^T, \tag{3a}$$

$$|1\rangle = |1\rangle_{\mathrm{L}} \otimes |\boldsymbol{b}\rangle = \Big(\underbrace{0 \cdots 0}_{n} b_1 \cdots b_n\Big)^T, \tag{3b}$$

where $|0\rangle_{\rm L} = (1, 0)^T$ and $|1\rangle_{\rm L} = (0, 1)^T$ are the 'logical components' of the logical basis states and $|\boldsymbol{a}\rangle$ and $|\boldsymbol{b}\rangle$ are the 'encoded components'. It follows that $\langle 0|0\rangle = \langle 1|1\rangle = 1$ and $\langle 0|1\rangle = 0$. Thus, any superposition state $|\psi\rangle$ can be written as

$$|\psi\rangle = c_0|0\rangle + c_1|1\rangle = c_0|0\rangle_{\rm L} \otimes |\boldsymbol{a}\rangle + c_1|1\rangle_{\rm L} \otimes |\boldsymbol{b}\rangle, \tag{4}$$

where $|\psi\rangle$ is a vector of dimension $2n$ and $|c_0|^2 + |c_1|^2 = 1$ so that $\langle\psi|\psi\rangle = 1$. Throughout this work we employ the following abbreviated notation:

$$|\psi\rangle = \begin{pmatrix} \alpha \\ \beta \end{pmatrix}, \tag{5}$$

where $\alpha = c_0|\boldsymbol{a}\rangle$ and $\beta = c_1|\boldsymbol{b}\rangle$.

There are many different physical situations in which a TPS in the form of (4) can be realized [42]. An important point is that in the case of MLE this TPS is *virtual* since it does not arise from spatially separated degrees of freedom, instead it is an abstract partitioning of the Hilbert space. This essential feature makes MLE physically quite different from the mathematically similar structure of quantum error correction (QEC) [43]. In the case of QEC one deals with a number of distinct physical systems (a qubit and ancillae) which become entangled via a set of controlled interactions between them. However, in the context of MLE we deal with a single quantum system for each qubit (even if this system is in fact composed of many particles, e.g., a molecule), and use of the tensor product is a convenient mathematical description. The Hilbert space of a molecule or atom is just one example of a state space in which a virtual TPS can be built. Other, very general, mechanisms of producing a TPS come from superselection rules and the representation theory of algebras of observables [42]. Therefore, there is a plethora of possibilities for building an MLE structure: from single atoms to molecules, to complex multiparticle systems.

As seen from (3*a*) and (4), different physical states, i.e., different choices of $|\boldsymbol{a}\rangle$ and $|\boldsymbol{b}\rangle$, can represent the same logical state. In order to rigorously formulate this principle of logical equivalence, we introduce a set of 'equivalence assay' (EA) operators:

$$\Lambda_x = \frac{1}{2}\sum_{i=1}^{n}(|\chi_i\rangle\langle\phi_i| + |\phi_i\rangle\langle\chi_i|), \tag{6a}$$

$$\Lambda_y = \frac{1}{2i}\sum_{i=1}^{n}(|\chi_i\rangle\langle\phi_i| - |\phi_i\rangle\langle\chi_i|), \tag{6b}$$

$$\Lambda_z = \frac{1}{2}\sum_{i=1}^{n}(|\chi_i\rangle\langle\chi_i| - |\phi_i\rangle\langle\phi_i|). \tag{6c}$$

The EA operators can also be rewritten in the matrix form

$$\Lambda_r = \lambda_r \otimes \mathbb{1}_n = \tfrac{1}{2}\sigma_r \otimes \mathbb{1}_n, \qquad r = \{x, y, z\}, \tag{7}$$

where $\{\sigma_x, \sigma_y, \sigma_z\}$ are the three Pauli matrices, $\{\lambda_x, \lambda_y, \lambda_z\}$ are the 2×2 matrices ($\lambda_r = \frac{1}{2}\sigma_r$) which represent the three generators of the SU(2) group, and $\mathbb{1}_n$ is the $n \times n$ identity matrix.

Expectation values of the EA operators of an arbitrary state $|\psi\rangle$ are

$$\langle\psi|\Lambda_x|\psi\rangle = \mathrm{Re}(c_0^* c_1 \langle \boldsymbol{a}|\boldsymbol{b}\rangle) = \mathrm{Re}(\alpha^\dagger \beta), \tag{8a}$$

$$\langle\psi|\Lambda_y|\psi\rangle = \mathrm{Im}(c_0^* c_1 \langle \boldsymbol{a}|\boldsymbol{b}\rangle) = \mathrm{Im}(\alpha^\dagger \beta), \tag{8b}$$

$$\langle\psi|\Lambda_z|\psi\rangle = \tfrac{1}{2}(|c_0|^2\langle \boldsymbol{a}|\boldsymbol{a}\rangle - |c_1|^2\langle \boldsymbol{b}|\boldsymbol{b}\rangle) = \tfrac{1}{2}(|c_0|^2 - |c_1|^2). \tag{8c}$$

Two physical states, $|\psi\rangle$ and $|\psi'\rangle$, are logically equivalent, which is denoted as $|\psi\rangle \sim |\psi'\rangle$, if they satisfy

$$\langle\psi|\Lambda_r|\psi\rangle = \langle\psi'|\Lambda_r|\psi'\rangle, \qquad r = \{x, y, z\}. \tag{9}$$

In addition, the states must be normalized ($\langle\psi|\psi\rangle = \langle\psi|\mathbb{1}_2 \otimes \mathbb{1}_n|\psi\rangle = 1$ for all $|\psi\rangle$). Logical equivalence resulting from MLE is analogous to equality in the context of SLE. Since the encoded component of all EA operators is the identity operator $\mathbb{1}_n$, logical equivalence, as defined by (9), allows for significant freedom in the choice of the encoded components of a state without making it logically different. On the other hand, the logical components of the EA operators, σ_r, together with the identity operator $\mathbb{1}_2$, span the space of all 2×2 matrices, ensuring that all equivalent states are logically the same, i.e. that no logical operation can distinguish between them.

Logical equivalence is a transitive property, i.e., if $|\psi\rangle \sim |\psi'\rangle$ and $|\psi\rangle \sim |\psi''\rangle$, then $|\psi'\rangle \sim |\psi''\rangle$. Therefore, all states which are mutually equivalent form an equivalence class $\mathcal{E}_\psi$, which is formally expressed as

$$\mathcal{E}_\psi = \{|\psi_s\rangle : |\psi_s\rangle \sim |\psi\rangle\}. \tag{10}$$

Correspondingly, every physical state in a given equivalence class represents the *same* logical state.

Logical equivalence can also be extended to quantum operations. Two operations, U and U' are logically equivalent (denoted as $U \sim U'$), if

$$U|\psi\rangle \sim U'|\psi\rangle \quad \text{for any } |\psi\rangle. \tag{11}$$

Logical equivalence for operations is also a transitive property, i.e., if $U \sim U'$ and $U \sim U''$, then $U' \sim U''$. Therefore, all physical transformations which are mutually equivalent form an equivalence class and every transformation in that class represents the *same* logical operation.

3. Single-qubit operations for MLE

Any 2×2 unitary matrix can be represented as a linear combination of the identity matrix $\mathbb{1}_2$ and the three Pauli matrices $\{\sigma_x, \sigma_y, \sigma_z\}$. The Pauli matrices (up to a numerical factor) are the generators of the Lie group SU(2) and satisfy a set of commutation and multiplication properties. Single-qubit logical operations for SLE are represented by elements of the U(2) group. In this section, we develop the corresponding representation of single-qubit logical operations within the context of MLE.

Using the partitioning scheme for logical basis states described in section 2, the general form of a unitary operation acting on a qubit encoded in the expanded $(2n)$-dimensional space is

$$U = \begin{pmatrix} A & B \\ C & D \end{pmatrix}, \tag{12}$$

where each sub-block A, B, C and D is an $n \times n$ matrix representing operations on and between the two encoding subspaces, $\mathcal{S}_0$ and $\mathcal{S}_1$. Note that any operation U is defined up to an overall phase factor.

3.1. The weak identity operation

The *weak* identity operation, U_I, is defined by the following property: under the conditions of logical equivalence, U_I leaves the equivalence class $\mathcal{E}_\psi$ invariant, i.e., $U_I\mathcal{E}_\psi = \mathcal{E}_\psi$, which can be expressed as

$$U_I|\psi\rangle \sim |\psi\rangle \quad \text{for any } |\psi\rangle. \tag{13}$$

Using the general decomposition of (12), the equation above is recast in the form

$$\begin{pmatrix} A\alpha + B\beta \\ C\alpha + D\beta \end{pmatrix} \sim \begin{pmatrix} \alpha \\ \beta \end{pmatrix}. \tag{14}$$

We find the explicit form of U_I by using the conditions of logical equivalence (9). The condition for Λ_z, combined with the normalization property, requires that

$$(\alpha^\dagger A^\dagger + \beta^\dagger B^\dagger)(A\alpha + B\beta) = \alpha^\dagger\alpha, \tag{15a}$$

$$(\alpha^\dagger C^\dagger + \beta^\dagger D^\dagger)(C\alpha + D\beta) = \beta^\dagger\beta, \tag{15b}$$

which is true if A and D are unitary and $B = C = 0$. Using these results, we next consider the two other conditions for equivalence (Λ_x and Λ_y):

$$\alpha^\dagger A^\dagger D\beta \pm \beta^\dagger D^\dagger A\alpha = \alpha^\dagger\beta \pm \beta^\dagger\alpha, \tag{16}$$

which are satisfied if $A = D$. Therefore, we obtain

$$U_I = \begin{pmatrix} V_0 & 0 \\ 0 & V_0 \end{pmatrix} = \mathbb{1}_2 \otimes V_0, \tag{17}$$

where V_0 is an arbitrary $n \times n$ unitary matrix and 0 denotes the $n \times n$ matrix of zeros. Therefore, the weak identity U_I is in fact a class of logically equivalent operations:

$$U_I = \{\mathbb{1}_2 \otimes V_0 : V_0 \in \mathrm{U}(n)\}. \tag{18}$$

The identity operation $\mathbb{1}_{2n}$ is also a member of this equivalence class (corresponding to $V_0 = \mathbb{1}_n$).

The notion of the weak identity operation clarifies the meaning of logical equivalence between different physical states. For any state $|\psi\rangle = (\alpha, \beta)^T$, the equivalence class $\mathcal{E}_\psi$ is

generated by the set of unitary operations U_I acting on $|\psi\rangle$:

$$\mathcal{E}_\psi = \{(\mathbb{1}_2 \otimes V_0)|\psi\rangle : V_0 \in \mathrm{U}(n)\}. \tag{19}$$

It is impossible to preserve logical equivalence when different transformations act on α and β, e.g., the state $|\tilde{\psi}\rangle = (V\alpha, V'\beta)^T$ with $V' \neq V$ is logically different from the state $|\psi\rangle = (\alpha, \beta)^T$ since the relative phase between $|0\rangle$ and $|1\rangle$ is changed. This is why the TPS of (17) is necessary for maintaining logical equivalence and emphasizes why logical equivalence is defined for a superposition state $|\psi\rangle$. It would be meaningless to define logical equivalence for the individual logical basis states since no definite relative phase between $|0\rangle$ and $|1\rangle$ would exist.

It follows from (19) that an infinite number of different physical states within an equivalence class correspond to the infinite number of different choices for the unitary transformation V_0. There also exists an infinite set of equivalence classes $\mathcal{E}_\psi$ themselves. If $|\psi_1\rangle = (\alpha_1, \beta_1)^T$ and $|\psi_2\rangle = (\alpha_2, \beta_2)^T$ are such that $U_I|\psi_1\rangle \neq |\psi_2\rangle$ for any choice of V_0, then the two equivalence classes $\mathcal{E}_{\psi_1}$ and $\mathcal{E}_{\psi_2}$ are distinct and have no common states. Theoretically there is no preference as to what equivalence class to use for MLE of a qubit; however, in a practical situation some specific equivalence class will be selected, for example, depending on the initial state of the qubit physical system or the technical limitations of the available controls.

3.2. The Pauli matrices

We will denote the high-dimensional representations of the Pauli matrices $\{\sigma_x, \sigma_y, \sigma_z\}$ as $\{U_x, U_y, U_z\}$. The construction of these operations for a multilevel-encoded qubit is similar to that of U_I. In particular, the form of the bit-flip operation U_x (the NOT gate) under the condition of logical equivalence is

$$U_x = \begin{pmatrix} 0 & V_1 \\ V_1 & 0 \end{pmatrix} = \sigma_x \otimes V_1, \tag{20}$$

where V_1 is an arbitrary $n \times n$ unitary matrix. It is easy to verify that

$$U_x|\psi\rangle = \begin{pmatrix} V_1\beta \\ V_1\alpha \end{pmatrix} \sim \begin{pmatrix} \beta \\ \alpha \end{pmatrix}. \tag{21}$$

As demonstrated in (21), U_x performs the desired bit-flip operation. Analogously, the other two Pauli matrices U_y and U_z (the latter being the phase-flip operation) have the form

$$U_y = \begin{pmatrix} 0 & -iV_2 \\ iV_2 & 0 \end{pmatrix} = \sigma_y \otimes V_2 \tag{22}$$

and

$$U_z = \begin{pmatrix} V_3 & 0 \\ 0 & -V_3 \end{pmatrix} = \sigma_z \otimes V_3, \tag{23}$$

where V_2 and V_3 are also arbitrary $n \times n$ unitary matrices. Under logical equivalence, the multiplication rule $\sigma_j = i\epsilon_{jkl}\sigma_k\sigma_l$ (where $\{j, k, l\} = \{x, y, z\}$ and ϵ_{jkl} is the completely antisymmetric unit tensor) and the anti-commutation rule $\{\sigma_j, \sigma_k\} = 0$ $(j \neq k)$ for the Pauli

matrices are expressed as

$$U_j \sim i\epsilon_{jkl} U_k U_l, \qquad \{j,k,l\} = \{x,y,z\} \tag{24a}$$

$$U_j U_k \sim -U_k U_j \qquad (j \neq k), \tag{24b}$$

respectively. One can easily verify that these relations are satisfied given the form of U_x, U_y and U_z and the arbitrary nature of V_1, V_2 and V_3.

3.3. The Hadamard gate

We denote the high-dimensional representation of the Hadamard gate H as U_H. Since $H\sigma_z H = \sigma_x$, U_H must satisfy $U_H U_z U_H|\psi\rangle \sim U_x|\psi\rangle$ for any $|\psi\rangle$. Consider U_H of the most general form of (12):

$$\begin{pmatrix} AV_3A - BV_3C & AV_3B - BV_3D \\ CV_3A - DV_3C & CV_3B - DV_3D \end{pmatrix}\begin{pmatrix}\alpha\\ \beta\end{pmatrix} \sim \begin{pmatrix}\beta\\ \alpha\end{pmatrix}, \tag{25}$$

which is true if $A = B = C = -D$ and $\sqrt{2}A$ is unitary. Therefore, U_H has the form

$$U_H = \frac{1}{\sqrt{2}}\begin{pmatrix} V_4 & V_4 \\ V_4 & -V_4 \end{pmatrix} = H \otimes V_4, \tag{26}$$

where V_4 is an arbitrary $n \times n$ unitary matrix.

3.4. The phase-shift gate

We denote the high-dimensional representation of the phase-shift gate $P(\phi)$ as $U_P(\phi)$, which has the form

$$U_P(\phi) = \begin{pmatrix} V_5 & 0 \\ 0 & V_5 e^{i\phi} \end{pmatrix} = P(\phi) \otimes V_5, \tag{27}$$

where $\phi \in \mathbb{R}$ and V_5 is an arbitrary $n \times n$ unitary matrix.

3.5. Weak commutation

Under logical equivalence, we can introduce a *weak* commutation relation. Two operators F and G are said to weakly commute if

$$FG \sim GF. \tag{28}$$

Within the MLE formalism, every logical operation should weakly commute with U_I (the weak identity). It is not difficult to see that U_I weakly commutes with the logical operations U_x, U_y, U_z, U_H and $U_P(\phi)$ described above. Moreover, we show that U_I weakly commutes with any unitary operation U_ξ such that

$$U_\xi \in \mathrm{U}(2) \otimes \mathrm{U}(n), \tag{29}$$

which is a subgroup of U($2n$). In order to prove that

$$U_I U_\xi \sim U_\xi U_I, \tag{30}$$

first note that any such operation can be written as $U_\xi = \xi \otimes V$, where $\xi \in \mathrm{U}(2)$ and $V \in \mathrm{U}(n)$. Then we find that

$$\langle\psi|U_\xi^\dagger U_I^\dagger \Lambda_r U_I U_\xi|\psi\rangle = \mathrm{Tr}((\xi^\dagger \lambda_r \xi) \otimes \mathbb{1}_n |\psi\rangle\langle\psi|) \tag{31}$$

and

$$\langle\psi|U_I^\dagger U_\xi^\dagger \Lambda_r U_\xi U_I|\psi\rangle = \mathrm{Tr}((\xi^\dagger \lambda_r \xi) \otimes \mathbb{1}_n |\psi\rangle\langle\psi|), \tag{32}$$

where

$$V_0^\dagger V^\dagger V V_0 = V^\dagger V_0^\dagger V_0 V = \mathbb{1}_n \tag{33}$$

for any unitary V_0 and V. Since the right-hand sides of (31) and (32) are equal, their left-hand sides must be equal as well, which concludes the proof of (30). Additionally, if an operation U_ξ weakly commutes with U_I, i.e., $U_I U_\xi \sim U_\xi U_I$, then U_ξ is an element of $\mathrm{U}(2) \otimes \mathrm{U}(n)$.

3.6. Comments and remarks

Due to the arbitrary nature of the encoded component V ($V \in \mathrm{U}(n)$), every logical operation is represented in the $(2n)$-dimensional space by an infinite number of logically equivalent transformations $U_\xi = \xi \otimes V$ (which collectively form an equivalence class characterized by ξ). Therefore, the use of MLE of logical basis states allows for a great flexibility in the choice of the actual physical transformation that realizes the desired logical operation, which can be an important advantage in many practical situations.

An interesting question is whether the flexibility in the encoded component of U_ξ makes it easier to find an optimal control field that produces a physical transformation belonging to the desired equivalence class of logical operations. The answer is not yet clear since ξ, the logical component of U_ξ, must still be produced with the same accuracy as in the single-level representation. Another question for future research is whether the flexibility due to the logical equivalence of different physical transformations improves the robustness of logical operations against noise in controls.

A restriction in the MLE formalism presented above is the requirement that both logical basis states, $|0\rangle$ and $|1\rangle$, are encoded by the same number of physical levels. Satisfying this requirement in a real physical system can sometimes be a difficult task. Consider for example, a logical basis encoded into vibrational levels on two electronic surfaces of a molecule. If the difference between the two vibrational frequencies is sufficiently large, a laser pulse of a given spectral width will encompass a different number of vibrational levels on the two surfaces. Therefore, it is necessary to consider how restricting the encoding subspaces to be of equal dimension can be dealt with in practice. First note that in any practical situation it is impossible to achieve the target quantum operation *exactly*. Correspondingly, laboratory controls are designed to produce an operation which is as close as possible to the target (an optimal control problem). In the case of SLE, the actual quantum operation should be as close as possible to the 2×2 target operation ξ. Analogously, in the case of MLE, the actual quantum operation should be as

close as possible to the $(2n) \times (2n)$ target operation $U_\xi = \xi \otimes V$ (with the additional flexibility provided by the arbitrary nature of V). Consider now what will happen if in reality one logical basis state is encoded into n levels and the other into $m = n + k$ levels ($k > 0$). In such a case the actual operation will be represented by an $(n + m) \times (n + m)$ unitary matrix U_{lab}, and the target operation should be of the form

$$U_{\text{target}} = (\xi \otimes V) \oplus W, \tag{34}$$

where W is an arbitrary $k \times k$ unitary matrix (this mathematical structure also frequently appears in the context of QEC and operator QEC, e.g., see [43, 44]). The physical meaning of this target operation is that a qubit encoded in the $(2n)$-dimensional space should not couple to the additional k levels. So the laboratory task is to design controls which will produce the actual operation U_{lab} as close as possible to U_{target} of (34). This is an optimal control problem which is not different *in principle* from the one encountered when $n = m$. Of course, the practical difficulty of finding optimal control fields can increase when the encoding subspaces have different dimensions, but the method of closed-loop laboratory control with shaped laser pulses is well suited for dealing with such problems. Moreover, one can argue that optimal control could benefit from freedom in the choice of the actual parcelling of the vibrational levels between the two subspaces since the experimenter does not have to *a priori* define the levels into pre-assigned groups. The most effective partitioning of physical levels into the logical basis can be included as part of the optimal control problem, with this additional freedom providing a potential for better solutions.

4. MLE for mixed states

The principle of logical equivalence can be extended to mixed states. Consider a density matrix that represents a state in the expanded $(2n)$-dimensional Hilbert space:

$$\rho = \sum_{i,j=1}^{2} (r_{ij}|i\rangle_{\text{LL}}\langle j|) \otimes R_{ij} = \begin{pmatrix} r_{11}R_{11} & r_{12}R_{12} \\ r_{21}R_{21} & r_{22}R_{22} \end{pmatrix}, \tag{35}$$

where r_{ij} are matrix elements representing the state of the logical component and R_{ij} are $n \times n$ matrices representing the state of the encoded component. As a density matrix, ρ has certain fundamental properties: $\rho = \rho^\dagger$, $\langle\psi|\rho|\psi\rangle \geqslant 0$ for all $|\psi\rangle$, and $\text{Tr}\,(\rho) = 1$. In appendix, we show that the logical-component matrix

$$\rho_{\text{L}} = \begin{pmatrix} r_{11} & r_{12} \\ r_{21} & r_{22} \end{pmatrix} \tag{36}$$

as well as the diagonal sub-blocks R_{11} and R_{22} also have these properties and thus are proper density matrices.

Logical equivalence for two density matrices ρ and ρ' is defined as

$$\text{Tr}(\rho\Lambda_r) = \text{Tr}(\rho'\Lambda_r), \qquad r = \{x, y, z\}, \tag{37}$$

plus the normalization condition $\text{Tr}\,(\rho) = \text{Tr}\left(\rho'\right) = 1$. Two unitary operations U_1 and U_2 are logically equivalent if they satisfy

$$U_1\rho U_1^\dagger \sim U_2\rho U_2^\dagger. \tag{38}$$

By evaluating the corresponding traces, it is straightforward to show that for the weak identity U_I,

$$\rho \sim U_I \rho U_I^\dagger \tag{39}$$

and

$$U_I U_\xi \rho U_\xi^\dagger U_I^\dagger \sim U_\xi U_I \rho U_I^\dagger U_\xi^\dagger \quad \text{for any } U_\xi \in \mathrm{U}(2) \otimes \mathrm{U}(n), \tag{40}$$

which is completely analogous to the result obtained for pure states in the previous section.

Now we investigate the process of *non-unitary* evolution (e.g., due to environmentally induced decoherence) in the context of MLE. We restrict our consideration to processes which are unitary in the logical component and general (not necessarily unitary) in the encoded component. Quantum operations (acting on the reduced density matrix ρ of the system of interest) representing such processes will be symbolically denoted as $\mathcal{L}_\xi \equiv \{\xi, \mathcal{W}\}$, where ξ, the logical component, is a 2×2 unitary matrix and $\mathcal{W}$, the encoded component, is a generalized quantum operation whose properties will be determined below. The action of $\mathcal{L}_\xi$ on ρ is represented as

$$\mathcal{L}_\xi \rho = \sum_{i,j=1}^{2} \xi(r_{ij}|i\rangle_{\mathrm{LL}}\langle j|)\xi^\dagger \otimes (\mathcal{W}R_{ij}). \tag{41}$$

Using the explicit matrix form of ξ, this can be rewritten as

$$\mathcal{L}_\xi \rho = \sum_{i,j,k,l=1}^{2} (\xi_{ij} r_{jk} \xi_{lk}^* |i\rangle_{\mathrm{LL}}\langle l|) \otimes (\mathcal{W}R_{jk}). \tag{42}$$

Since $\mathcal{L}_\xi$ and $\mathcal{W}$ act on the density matrices ρ and $\{R_{ii}\}$, respectively, these operations must preserve Hermiticity, positivity and the trace. Therefore, a permissible operation $\mathcal{W}$ is a positive and trace-preserving map.

Next, consider the effect of the generalized weak identity, $\mathcal{L}_I = \{\mathbb{1}_2, \mathcal{W}\}$, on ρ:

$$\rho' = \mathcal{L}_I \rho = \sum_{i,j=1}^{2} (r_{ij}|i\rangle_{\mathrm{L}\ \mathrm{L}}\langle j|) \otimes (\mathcal{W}R_{ij}). \tag{43}$$

Using the explicit form of the EA operators,

$$\Lambda_r = \lambda_r \otimes \mathbb{1}_n = \sum_{i,j=1}^{2} \lambda_{ij}^{(r)} |i\rangle_{\mathrm{L}\ \mathrm{L}}\langle j| \otimes \mathbb{1}_n, \tag{44}$$

we obtain

$$\mathrm{Tr}(\rho' \Lambda_r) = \sum_{i,j=1}^{2} r_{ij} \lambda_{ji}^{(r)} \mathrm{Tr}(\mathcal{W}R_{ij}) = \sum_{i,j=1}^{2} r_{ij} \lambda_{ji}^{(r)} \mathrm{Tr}(R_{ij}) = \mathrm{Tr}(\rho \Lambda_r), \tag{45}$$

where we used the fact that $\mathcal{W}$ is a trace-preserving operation. This proves that $\mathcal{L}_I$ indeed has the property of the weak identity:

$$\mathcal{L}_I \rho \sim \rho. \tag{46}$$

An immediate and interesting consequence of (46) is the logical equivalence of mixed and pure states. In other words, while $\rho_\psi = |\psi\rangle\langle\psi|$ represents a pure state in the form of (4), its logically equivalent state $\rho' = \mathcal{L}_I \rho_\psi$ will be mixed if $\mathcal{L}_I$ includes any permissible and non-unitary operation $\mathcal{W}$. Thus, a logical basis state can be encoded into a subspace of multiple physical levels which are mixed (e.g., by a thermal excitation) without any loss of coherence *between* the two logical basis states that form a qubit. For example, if an initial state is such that mixing is only *within* an encoding subspace and not *between* the two subspaces, then quantum computation with MLE can be conducted without any loss of fidelity due to intra-subspace mixing. This property makes the method of MLE a very promising practical alternative to the cumbersome process of ground-state cooling.

An additional property of $\mathcal{W}$ is found by examining the weak commutation relation. Applying the method of proof used in (31) and (32) to general quantum operations in the form of (41), it follows that any permissible operation $\mathcal{L}_\xi$ weakly commutes with $\mathcal{L}_I$, i.e.,

$$\mathcal{L}_I \mathcal{L}_\xi \rho \sim \mathcal{L}_\xi \mathcal{L}_I \rho, \tag{47}$$

if

$$\mathrm{Tr}(\mathcal{W}_0 \mathcal{W} R_{ij}) = \mathrm{Tr}(\mathcal{W} \mathcal{W}_0 R_{ij}) \quad \text{for all } i,\ j. \tag{48}$$

Here, $\mathcal{W}_0$ and $\mathcal{W}$ are the encoded components of $\mathcal{L}_I$ and $\mathcal{L}_\xi$, respectively. Equations (47) and (48) show that all permissible operations $\{\mathcal{W}\}$ form a closed set. In other words, if $\mathcal{W}$ and $\mathcal{W}'$ are two arbitrary permissible operations, then $\mathcal{W}'' = \mathcal{W}\mathcal{W}'$ is another permissible operation. An example of a positive and trace-preserving map with this closure property is the Kraus representation:

$$\mathcal{W} R_{ij} = \sum_\nu W_\nu R_{ij} W_\nu^\dagger, \qquad \text{where } \sum_\nu W_\nu^\dagger W_\nu = \mathbb{1}_n, \tag{49}$$

which is in fact a *completely* positive map [1].

It is now possible to generalize the notion of a class of logically equivalent operations to non-unitary processes. For each logical component $\xi \in \mathrm{U}(2)$, there exists an infinite number of equivalent logical operations $\mathcal{L}_\xi$ (forming an equivalence class) which permit decoherence *within* an encoding subspace but preserve coherence *between* the encoding subspaces. Specifically, any two operations $\mathcal{L}_\xi = \{\xi, \mathcal{W}\}$ and $\mathcal{L}'_\xi = \{\xi, \mathcal{W}'\}$, with permissible maps $\mathcal{W}$ and $\mathcal{W}'$, are logically equivalent (also illustrating that a non-unitary operation $\mathcal{L}_\xi = \{\xi, \mathcal{W}\}$ is logically equivalent to a unitary operation $U_\xi = \xi \otimes V$, where $V \in \mathrm{U}(n)$). Accordingly, MLE allows for quantum computation with full fidelity in the presence of non-unitary evolution within the encoding subspaces.

5. Example: numerical simulation of closed-loop optimal control of unitary operations in a multilevel system

To illustrate the formalism and advantages of MLE, as developed in sections 2–4, we perform a simulation of closed-loop optimal control of single-qubit unitary operations for a model system. It should be emphasized that the method of closed-loop optimal control is uniquely suited for laboratory implementation, but is very difficult to simulate on the computer, except for the

simplest models. This is related to the fact that learning algorithms (e.g., genetic algorithms) which are used to search for the optimal control fields, involve vast amounts of data processing. In our numerical simulations, solving the time-dependent Schrödinger equation for each set of control parameters is the limiting computational step. Since a learning algorithm typically needs to search over hundreds of thousands or even millions of points in the parameter space until a global optimum is found, the simulation can take days even for relatively simple model systems. However, in the laboratory, a real physical system, whatever complex it may be, 'solves' its own time-dependent Schrödinger equation in real time. Hence, the data processing of the learning algorithm in the laboratory is limited mainly by the repetition rate of the laser and pulse-shaping system, which can be as fast as several kilohertz and consequently, the search over a million of different control fields can be completed in just several minutes.

5.1. The model

Due to the previous considerations, we perform just a proof-of-principle numerical simulation of optimal control for a simple four-level model system which nevertheless demonstrates the difference between the MLE and SLE operations in the presence of decoherence. This model represents a single qubit with each logical basis state encoded either by two levels in the case of MLE ($n = 2$) or by one level in the case of SLE (the other two levels remain unused). The energy spacings correspond to the electronic and vibrational levels of the sodium dimer, Na_2.[6] For MLE, the ground and excited electronic states correspond to the $|0\rangle$ and $|1\rangle$ logical basis states, respectively, i.e., each logical basis state is encoded by a pair of vibrational levels on the corresponding electronic surface. For SLE, the logical basis states $|0\rangle$ and $|1\rangle$ are defined as the lower vibrational levels on the ground and excited electronic surfaces, respectively. In a homonuclear dimer such as Na_2, transitions between vibrational levels within a given electronic surface are forbidden (the dipole moment for these transitions is zero). Transitions between different electronic surfaces are allowed and correspond to the dipole moment set to unity. Thus, the number of allowed transitions equals n^2.

Unary multilevel atomic and molecular systems, such as Na_2, are not scalable for quantum computing applications in the absence of physical entanglement. Implementations of quantum algorithms without entanglement have been investigated using Rydberg atoms [46, 47] and linear optical systems [48]–[50]. It was concluded that quantum computation with a single multilevel system is possible, but requires exponentially greater overhead than a multiparticle quantum computer that operates with entanglement [51, 52]. Therefore, there exists significant interest in engineering interactions between atoms or molecules for creating entanglement needed for efficient and scalable quantum information processing [53]–[62]. However, in our example scalability is not the issue, as we use the model multilevel system to investigate some of the most basic features of MLE for a single qubit.

There exist plans to use homonuclear dimers such as Na_2 and K_2 for experimentally studying the basic functioning of MLE in single-qubit systems in the presence of thermalization. These experiments would benefit from existing technologies for managing and measuring the dynamics of vibrational molecular wavepackets [25, 63], including applications of closed-loop control methods [64]. A much greater challenge would be an experimental realization of MLE in

[6] The energy separation between the ground and first excited electronic surfaces is 0.066889653 au; the separations between vibrational levels are 0.0007250238 and 0.000534563 au on the ground and excited electronic surfaces, respectively. The data are taken from [45].

entangled multi-qubit systems, such as photon-atom quantum memories, as the technology for this future type of experiments is not yet fully developed.

5.2. Formulation of the optimal control problem

The time evolution operator $U(t)$ for an isolated quantum system satisfies the Schrödinger equation:

$$\frac{\mathrm{d}}{\mathrm{d}t}U(t) = -\frac{i}{\hbar}H(t)U(t). \tag{50}$$

The time-dependent Hamiltonian, $H(t)$, in this model is

$$H(t) = H_0 - \mu\epsilon(t), \tag{51}$$

where H_0 is the system Hamiltonian in the absence of control, μ is the electric dipole-moment operator and $\epsilon(t)$ is the time-dependent control field, defined as

$$\epsilon(t) = f(t)\sum_{i=1}^{n^2} a_i \cos(\omega_i t + \delta_i). \tag{52}$$

Here, $f(t)$ is an envelope function which incorporates the laser pulse width (e.g., a Gaussian or similar type of distribution) and a_i, ω_i, δ_i are the amplitude, frequency and relative phase of the ith electric field component, respectively. Transition frequencies are determined by the system Hamiltonian. The operation is over the time interval $[0, t_f]$.[7]

The control objective is to achieve the time evolution operator $U(t_f)$ which is as close as possible to the target transformation U_{target}. The fitness of the control field is evaluated by using the gate fidelity, which is a functional of control:

$$\mathcal{F}[\epsilon(t)] = 1 - \|U_{\text{target}} - U(t_f)\|. \tag{53}$$

Optimal control solutions correspond to maxima of $\mathcal{F}$. The search for a global maximum is performed using a genetic algorithm (GA) implemented with population sizes of ∼200, several different reproductive schemes, and cross-over and mutation rates between 20 and 40%.

5.2.1. Fidelity functionals for MLE. For MLE, the specific matrix norm in (53) will depend on the target transformation. The general form of the unitary evolution operator $U(t_f)$ can be written as

$$U(t_f) = \begin{pmatrix} A & B \\ C & D \end{pmatrix}, \tag{54}$$

where A, B, C and D are square matrices of dimension n. For the bit-flip operation U_x of (20) and the phase-flip operation U_z of (23) as the target transformations, we use fidelity functionals

[7] In our simulations, t_f can vary from 2×10^3 to 5×10^4 au (i.e., from about 48 fs to 1.2 ps).

of the form

$$\mathcal{F}_x = 1 - \left(\frac{\|BB^\dagger - 1\|^2}{n} + \frac{\|B - C\|^2}{4n} \right)^{1/2} \tag{55}$$

and

$$\mathcal{F}_z = 1 - \left(\frac{\|AA^\dagger - 1\|^2}{n} + \frac{\|A + D\|^2}{4n} \right)^{1/2}, \tag{56}$$

respectively, where the matrix norm is defined as $\|M\|^2 = \mathrm{Tr}\left(MM^\dagger\right)$ and the coefficients are chosen for the proper normalization, so that $0 \leqslant \mathcal{F}_x \leqslant 1$ and $0 \leqslant \mathcal{F}_z \leqslant 1$. The maximum of the fidelity functional ($\mathcal{F}_x = 1$ or $\mathcal{F}_z = 1$) is achieved when the actual transformation $U(t_f)$ is an element of the corresponding equivalence class (U_x or U_z).

5.2.2. Fidelity functionals for SLE. For SLE, two vibrational levels are used to encode the logical basis states, while the other two levels are unused. Therefore, the bit-flip and the phase-flip operations are represented by the unitary transformations

$$U'_x = \sigma_x \oplus v \tag{57}$$

and

$$U'_z = \sigma_z \oplus w, \tag{58}$$

respectively, where σ_x and σ_z are the corresponding Pauli matrices acting on the space of the logical basis, and v and w are arbitrary 2×2 unitary matrices acting on the space of the two unused levels. For computations, we rearrange U'_x and U'_z so that their indices correspond to the physical order of the energy levels (the logical basis states $|0\rangle$ and $|1\rangle$ correspond to the 1st and 3rd energy levels, respectively). For the SLE operations U'_x and U'_z as the target transformations, the fidelity functional will be of the form

$$\mathcal{F}'_x = \tfrac{1}{2}|U_{13} + U_{31}| \tag{59}$$

and

$$\mathcal{F}'_z = \tfrac{1}{2}\,|U_{11} - U_{33}|\,, \tag{60}$$

respectively, where U_{ij} denotes the corresponding matrix element of the actual transformation $U(t_f)$. The maximum of the fidelity functional ($\mathcal{F}'_x = 1$ or $\mathcal{F}'_z = 1$) is achieved when the actual transformation $U(t_f)$ produces the target transformation (σ_x or σ_z, up to a global phase) in the two-level subspace of the logical basis.

Table 1. Fidelities of MLE and SLE logical operations using the GA optimization.

$\mathcal{F}_x$	$\mathcal{F}_z$	$\mathcal{F}'_x$	$\mathcal{F}'_z$
0.9987	0.9975	0.9998	0.9996

5.3. Numerical optimization and analysis of results

Table 1 summarizes the gate fidelities obtained from the GA optimization for MLE ($n = 2$) and SLE configurations of the four-level model system. The GA is capable of finding optimal control solutions for both MLE and SLE cases with reasonable accuracies, limited mainly by the parameterized structure of the control fields in (52). These fidelities could be improved by coupling the results of the GA to an additional gradient-based search algorithm that does not rely on any particular parameterization of the control fields. However, for the purposes of our simulations, the logical operations obtained with the GA were sufficient to demonstrate the main distinctions between MLE and SLE.

We are also interested to see what happens when we apply the optimal transformation located by GA optimization on an initial state which is mixed by a decoherence process (we assume that the effect of decoherence *during* the logical operation is negligible and that only the initial state is affected). We consider two types of decoherence processes: dephasing (only for MLE) and thermalization (for both MLE and SLE).

To investigate the effect of initial state decoherence on the fidelity of quantum operations, we consider the difference between the perfect (or intended) initial state rotated by the perfect target transformation:

$$\rho_{\text{target}} = U_{\text{target}} \rho U_{\text{target}}^{\dagger}, \tag{61}$$

and the actual initial state rotated by the optimal actual transformation found by the GA:

$$\rho(t_f) = U(t_f)\tilde{\rho}U(t_f)^{\dagger}. \tag{62}$$

The actual initial state $\tilde{\rho}$ may be affected by a decoherence process and therefore differ from the perfect initial state ρ. For MLE, the difference between ρ_{target} and $\rho(t_f)$ is estimated by evaluating the 'error of equivalence':

$$\varepsilon[\rho, \tilde{\rho}] = \tfrac{1}{3} \sum_{r=x,y,z} |\text{Tr}(\Lambda_r[\rho(t_f) - \rho_{\text{target}}])|, \tag{63}$$

where $\{\Lambda_x, \Lambda_y, \Lambda_z\}$ are the three EA operators of (7). This error measures how far the two density matrices are from complete logical equivalence. The worst value of ε is 1, while in the case of complete equivalence $\varepsilon = 0$. For SLE, the distance between the perfect target state and the actual final state is measured by

$$\varepsilon'[\rho, \tilde{\rho}] = \text{Tr}([\rho(t_f) - \rho_{\text{target}}]^2). \tag{64}$$

In the absence of decoherence ($\tilde{\rho} = \rho$), the errors ε and ε' will be nonzero only due to the fact that the optimal control solution found by the GA produces a transformation that is slightly

different from the target one. However, if decoherence impairs the initial state ($\tilde{\rho} \neq \rho$), this can significantly affect the error. We will see below that operations resulting from MLE are not at all hindered by dephasing or thermalization of the initial state. In contrast, the performance of SLE operations deteriorates if the initial state is thermalized.

5.3.1. MLE operations in the presence of dephasing. Dephasing of non-stationary vibrational wave packets in hot alkaline dimers is caused by the vibrational–rotational coupling [15]. The typical dephasing time is inversely proportional to the temperature and varies from ∼3 ps for very hot molecules (produced in a heat pipe at about 400 °C) to ∼20 ps for vapours cooled to about 100 K. Note that the decoherence time on the electronic surfaces (i.e., *within* the encoding subspaces of the MLE scheme) due to this coupling is much shorter than that *between* electronic surfaces associated with spontaneous emission from the excited electronic surface, which happens on the timescale of several nanoseconds. Therefore, dephasing induced by the vibrational–rotational coupling is the most important mechanism of decoherence for vibrational wave-packets. Since the length of the optimal control pulse does not exceed 1.2 ps (and can even be made shorter at the cost of a small decrease in the gate fidelity), the effect of dephasing *during* the logical operation is negligible at temperatures about 100 K.

We study the effect of dephasing on MLE operations by considering a set of randomly generated pure initial states of the form

$$|\psi\rangle = c_0|0\rangle_{\mathrm{L}} \otimes \begin{pmatrix} \cos(\theta_0) \\ \exp(i\phi_0)\sin(\theta_0) \end{pmatrix} + c_1|1\rangle_{\mathrm{L}} \otimes \begin{pmatrix} \cos(\theta_1) \\ \exp(i\phi_1)\sin(\theta_1) \end{pmatrix}, \tag{65}$$

where c_0, c_1, ϕ_0, ϕ_1, θ_0 and θ_1 are randomly generated real parameters such that

$$c_0^2 + c_1^2 = 1, \tag{66a}$$

$$0 \leqslant \phi_0, \phi_1, \theta_0, \theta_1 \leqslant 2\pi. \tag{66b}$$

The initial state $|\psi\rangle$ corresponds to the density matrix $\rho = |\psi\rangle\langle\psi|$, whose elements in the basis of the four energy levels are denoted as $\langle i|\rho|j\rangle = r_{ij}$ ($i, j = 1, 2, 3, 4$). Dephasing within each encoding subspace is represented by setting the off-diagonal matrix elements of each diagonal sub-block equal to zero, resulting in the mixed state

$$\tilde{\rho} = \begin{pmatrix} r_{11} & 0 & r_{13} & r_{14} \\ 0 & r_{22} & r_{23} & r_{24} \\ r_{31} & r_{32} & r_{33} & 0 \\ r_{41} & r_{42} & 0 & r_{44} \end{pmatrix}. \tag{67}$$

The error of equivalence for the U_x and U_z target transformations is evaluated both in the absence and in the presence of dephasing: $\varepsilon[\rho, \rho]$ and $\varepsilon[\rho, \tilde{\rho}]$, as defined in (63), and averaged over 10^6 random choices of the initial state $|\psi\rangle$ in the form of (65). These average errors, $\langle\varepsilon\rangle$, are presented in table 2. We see that the operation error does not increase (and even slightly decreases) when the initial state is affected by dephasing. This means that the pure state ρ and the dephased state $\tilde{\rho}$ are equally suitable for MLE operations due to their logical equivalence.

Table 2. Average errors of MLE operations with and without dephasing of the initial state.

Initial state	$\langle\varepsilon\rangle$ for U_x	$\langle\varepsilon\rangle$ for U_z
ρ	0.0093	0.0146
$\tilde{\rho}$	0.0076	0.0134

5.3.2. MLE and SLE operations in the presence of thermalization. As mentioned above, alkaline dimers are typically produced at high temperatures of up to 400°C. Moreover, these molecules are unstable at low temperatures, although vapours of sufficiently low concentrations can be carefully cooled to 100 K or even slightly below. We study the effect of thermalization on both MLE and SLE operations by considering the following pure initial state:

$$|\psi\rangle = |0\rangle_{\mathrm{L}} \otimes \begin{pmatrix} 1 \\ 0 \end{pmatrix} = (1, 0, 0, 0)^T, \tag{68}$$

which corresponds to the lowest energy state of the molecule. The resulting density matrix $\rho = |\psi\rangle\langle\psi|$ has only one nonzero element: $\langle i|\rho|j\rangle = \delta_{i1}\delta_{j1}$ $(i, j = 1, 2, 3, 4)$. Thermalization impairs the pure initial state of (68) and results in a mixed state $\tilde{\rho}$ of the form

$$\tilde{\rho} = \begin{pmatrix} 1-\Delta & 0 & 0 & 0 \\ 0 & \Delta & 0 & 0 \\ 0 & 0 & 0 & 0 \\ 0 & 0 & 0 & 0 \end{pmatrix}, \tag{69}$$

where $\Delta = \exp(-E_v/k_BT)$, k_B is the Boltzmann constant, T is the temperature, and E_v is the energy separation between the vibrational levels on the ground electronic surface. Thermal excitations to all energy levels higher than $|n_v = 1\rangle$ are neglected, which is a reasonable approximation at temperatures of about 100 K and below.

At zero temperature (i.e., when $\tilde{\rho} = \rho$), the errors of MLE and SLE bit-flip operations (as defined in (63) and (64), respectively) are $\varepsilon = 0.0097$ (for U_x) and $\varepsilon' = 0.0009$ (for U_x'), respectively. This is consistent with the fact that optimal controls found by the GA have a higher fidelity for the SLE operations in comparison with the MLE ones, as shown in table 1. However, the situation is strikingly different in the presence of thermalization. We evaluate the errors for both MLE and SLE operations, $\varepsilon[\rho, \tilde{\rho}]$ and $\varepsilon'[\rho, \tilde{\rho}]$, respectively, for the range of temperatures between 70 and 120 K (corresponding to values of Δ between approximately 0.037 and 0.129). These errors are shown in figure 2 versus the temperature. The error of the SLE operation increases quite rapidly with the temperature and at temperatures above 85 K the performance of the SLE operation is worse than that of the MLE one. This increase of the SLE operation error is explained by the fact that at higher temperatures a larger portion of the population is transferred out of the logical basis. On the other hand, the performance of the MLE operation changes very little with thermalization (in fact, the error of the MLE operations slightly decreases as the temperature increases). This is explained by the fact that the population transfer *within* the encoding subspace (caused by thermalization) does not affect the logical state of a qubit with MLE, as discussed in section 4. Thus, the pure state ρ and the thermalized state $\tilde{\rho}$ are equally suitable for the MLE operation due to their logical equivalence.

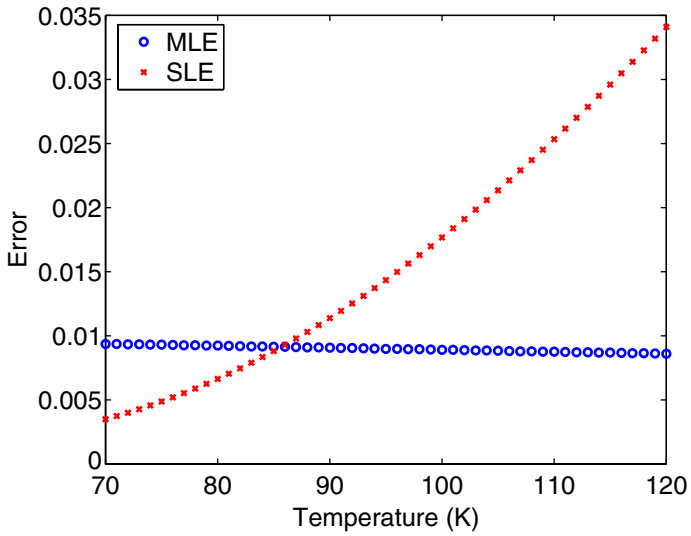

Figure 2. Errors of MLE and SLE bit-flip operations, $\varepsilon[\rho, \tilde{\rho}]$ of (63) and $\varepsilon'[\rho, \tilde{\rho}]$ of (64), respectively, for the thermalized initial state $\tilde{\rho}$ of (69), versus the temperature.

6. Two-qubit operations for MLE

For a two-qubit system, the formalism of MLE is analogous to that developed in the previous sections for a single qubit. As before, the energy levels of a quantum system realizing the kth qubit are divided into two distinct encoding subspaces of equal dimension, $\mathcal{S}_{0k}$ and $\mathcal{S}_{1k}$. Let $|\boldsymbol{a}\rangle_k$ denote *any* element of $\mathcal{S}_{0k}$ such that ${}_k\langle \boldsymbol{a}|\boldsymbol{a}\rangle_k = 1$ and $|\boldsymbol{b}\rangle_k$ denote *any* element of $\mathcal{S}_{1k}$ such that ${}_k\langle \boldsymbol{b}|\boldsymbol{b}\rangle_k = 1$, i.e.,

$$|\boldsymbol{a}\rangle_k = \sum_{i=1}^{n} a_{ik}|\chi_i\rangle_k = (a_{1k}\cdots a_{nk})^T, \qquad \text{such that} \sum_{i=1}^{n} |a_{ik}|^2 = 1 \tag{70}$$

and

$$|\boldsymbol{b}\rangle_k = \sum_{i=1}^{n} b_{ik}|\phi_i\rangle_k = (b_{1k}\cdots b_{nk})^T, \qquad \text{such that} \sum_{i=1}^{n} |b_{ik}|^2 = 1, \tag{71}$$

where $k \in \{1, 2\}$ denotes qubit 1 or qubit 2, n is the dimension of *all* encoding subspaces, and $\{|\chi_i\rangle_k\}$ and $\{|\phi_i\rangle_k\}$ are orthonormal bases that span $\mathcal{S}_{0k}$ and $\mathcal{S}_{1k}$, respectively. Correspondingly, ${}_k\langle \chi_i|\chi_j\rangle_{k'} = {}_k\langle \phi_i|\phi_j\rangle_{k'} = \delta_{ij}\delta_{kk'}$ and ${}_k\langle \chi_i|\phi_j\rangle_{k'} = 0$. Now the logical basis of the kth qubit is expressed as

$$|0\rangle_k = |0\rangle_{\mathrm{L}} \otimes |\boldsymbol{a}\rangle_k = \Big(a_{1k}\cdots a_{nk}\underbrace{0\cdots 0}_{n}\Big)^T, \tag{72a}$$

$$|1\rangle_k = |1\rangle_{\mathrm{L}} \otimes |\boldsymbol{b}\rangle_k = \Big(\underbrace{0\cdots 0}_{n} b_{1k}\cdots b_{nk}\Big)^T. \tag{72b}$$

It follows that ${}_k\langle 0|0\rangle_{k'} = {}_k\langle 1|1\rangle_{k'} = \delta_{kk'}$ and ${}_k\langle 0|1\rangle_{k'} = 0$. In the abbreviated notation,

$$|0\rangle_k = \begin{pmatrix} |\boldsymbol{a}\rangle_k \\ 0 \end{pmatrix}, \qquad |1\rangle_k = \begin{pmatrix} 0 \\ |\boldsymbol{b}\rangle_k \end{pmatrix}, \tag{73}$$

and the state vector for the kth qubit can be written as

$$|\psi\rangle_k = c_{0k}|0\rangle_k + c_{1k}|1\rangle_k = \begin{pmatrix} \alpha_k \\ \beta_k \end{pmatrix}, \tag{74}$$

where $|c_{0k}|^2 + |c_{1k}|^2 = 1$ (to ensure normalization) and $\alpha_k = c_{0k}|\boldsymbol{a}\rangle_k$ and $\beta_k = c_{1k}|\boldsymbol{b}\rangle_k$.

The logical basis of the two-qubit system can be defined as

$$|0\rangle_1 \otimes |0\rangle_2 = \begin{pmatrix} |\boldsymbol{a}\rangle_1 \\ 0 \end{pmatrix} \otimes \begin{pmatrix} |\boldsymbol{a}\rangle_2 \\ 0 \end{pmatrix}, \tag{75a}$$

$$|0\rangle_1 \otimes |1\rangle_2 = \begin{pmatrix} |\boldsymbol{a}\rangle_1 \\ 0 \end{pmatrix} \otimes \begin{pmatrix} 0 \\ |\boldsymbol{b}\rangle_2 \end{pmatrix}, \tag{75b}$$

$$|1\rangle_1 \otimes |0\rangle_2 = \begin{pmatrix} 0 \\ |\boldsymbol{b}\rangle_1 \end{pmatrix} \otimes \begin{pmatrix} |\boldsymbol{a}\rangle_2 \\ 0 \end{pmatrix}, \tag{75c}$$

$$|1\rangle_1 \otimes |1\rangle_2 = \begin{pmatrix} 0 \\ |\boldsymbol{b}\rangle_1 \end{pmatrix} \otimes \begin{pmatrix} 0 \\ |\boldsymbol{b}\rangle_2 \end{pmatrix}. \tag{75d}$$

However, it is much more convenient to use another basis, which is obtained by a unitary transformation on the basis defined above. The preferred logical basis for the two-qubit (TQ) system is

$$|1\rangle_{\mathrm{TQ}} = R\left(|0\rangle_1 \otimes |0\rangle_2\right) = \begin{pmatrix} |\boldsymbol{a}\rangle_1 \otimes |\boldsymbol{a}\rangle_2 \\ 0 \\ 0 \\ 0 \end{pmatrix}, \tag{76a}$$

$$|2\rangle_{\mathrm{TQ}} = R\left(|0\rangle_1 \otimes |1\rangle_2\right) = \begin{pmatrix} 0 \\ |\boldsymbol{a}\rangle_1 \otimes |\boldsymbol{b}\rangle_2 \\ 0 \\ 0 \end{pmatrix}, \tag{76b}$$

$$|3\rangle_{\mathrm{TQ}} = R\left(|1\rangle_1 \otimes |0\rangle_2\right) = \begin{pmatrix} 0 \\ 0 \\ |\boldsymbol{b}\rangle_1 \otimes |\boldsymbol{a}\rangle_2 \\ 0 \end{pmatrix}, \tag{76c}$$

$$|4\rangle_{\mathrm{TQ}} = R\left(|1\rangle_1 \otimes |1\rangle_2\right) = \begin{pmatrix} 0 \\ 0 \\ 0 \\ |\boldsymbol{b}\rangle_1 \otimes |\boldsymbol{b}\rangle_2 \end{pmatrix}, \tag{76d}$$

where R is a $4n^2 \times 4n^2$ unitary transformation. Now consider $|\Psi\rangle$, a state vector of the two-qubit system. In the logical basis of (76*a*), $|\Psi\rangle$ is expressed as

$$|\Psi\rangle = \sum_{i=1}^{4} c_i |i\rangle_{\mathrm{TQ}}, \tag{77}$$

where $\sum_{i=1}^{4} |c_i|^2 = 1$ ensures that $\langle\Psi|\Psi\rangle = 1$ ($|\Psi\rangle$ is a vector of dimension $4n^2$).

In order to formulate the principle of logical equivalence for the two-qubit system, we introduce a set of 15 EA operators,

$$\Lambda_r = \lambda_r \otimes \mathbb{1}_{n^2}, \qquad r = \{1, 2, \ldots, 15\}, \tag{78}$$

where $\mathbb{1}_{n^2}$ is the $n^2 \times n^2$ identity matrix and $\{\lambda_r\}$ is the set of 4×4 matrices which represent the 15 generators of SU(4), which, with $\mathbb{1}_4$, span the space of all 4×4 matrices. The principle of logical equivalence is formulated analogously to the single-qubit case. Two physical states, $|\Psi\rangle$ and $|\Psi'\rangle$, are logically equivalent (denoted as $|\Psi\rangle \sim |\Psi'\rangle$) if

$$\langle\Psi|\Lambda_r|\Psi\rangle = \langle\Psi'|\Lambda_r|\Psi'\rangle, \qquad r = \{1, 2, \ldots, 15\}. \tag{79}$$

Now we develop the explicit form of logical operations for the two-qubit system with MLE of the logical basis states. First, consider local operations which act separately on the two qubits. Such an operation is represented (in the preferred basis) by the matrix

$$U = R(U^{(1)} \otimes U^{(2)})R^{\dagger}, \tag{80}$$

where $U^{(k)}$ acts on the kth qubit. In particular, the weak identity operation that maintains logical equivalence for the entire two-qubit system and simultaneously for each of the individual qubits is given by

$$U_I = R(U_I^{(1)} \otimes U_I^{(2)})R^{\dagger} = \mathbb{1}_4 \otimes [V_0^{(1)} \otimes V_0^{(2)}], \tag{81}$$

where $U_I^{(k)}$ is the weak identity operation and $V_0^{(k)}$ is an arbitrary $n \times n$ unitary matrix acting on the kth qubit. As in the single-qubit case, the two-qubit weak identity satisfies

$$U_I|\Psi\rangle \sim |\Psi\rangle \text{ for any } |\Psi\rangle. \tag{82}$$

The proof given in (31) and (32) easily extends to the two-qubit case, so any operation U such that

$$U \in \mathrm{U}(4) \otimes [\mathrm{U}(n) \otimes \mathrm{U}(n)] \subset \mathrm{U}(4n^2) \tag{83}$$

satisfies $U_I U \sim U U_I$. Therefore, any two-qubit logical operation S resulting from SLE will be represented in the framework of MLE by a matrix of the form

$$U_S = S \otimes [V^{(1)} \otimes V^{(2)}], \tag{84}$$

where $S \in \mathrm{U}(4)$ and $V^{(k)} \in \mathrm{U}(n)$. Since $V^{(1)}$ and $V^{(2)}$ are arbitrary unitary matrices, any logical operation will be represented by an infinite number of logically equivalent physical transformations.

The tensor-product form $V^{(1)} \otimes V^{(2)}$ of (84) is required in order to ensure that entanglement created by a logical operation is reversible not only by a specific inverse operation, but by any member of a class of logically equivalent operations. To demonstrate this point, consider the C-NOT gate, U_{CN}. For MLE, this operation is represented by the following set of logically equivalent $(4n^2) \times (4n^2)$ matrices:

$$U_{\mathrm{CN}} = \begin{pmatrix} 1 & 0 & 0 & 0 \\ 0 & 1 & 0 & 0 \\ 0 & 0 & 0 & 1 \\ 0 & 0 & 1 & 0 \end{pmatrix} \otimes [V^{(1)} \otimes V^{(2)}]$$

$$= \begin{pmatrix} V^{(1)} \otimes V^{(2)} & 0 & 0 & 0 \\ 0 & V^{(1)} \otimes V^{(2)} & 0 & 0 \\ 0 & 0 & 0 & V^{(1)} \otimes V^{(2)} \\ 0 & 0 & V^{(1)} \otimes V^{(2)} & 0 \end{pmatrix}. \tag{85}$$

Equation (85) defines an entire class of logically equivalent operations. With SLE, applying the C-NOT operation twice results in the identity operation. Thus, applying the operation U_{CN} twice should result in a logically equivalent state, i.e.,

$$U_{\mathrm{CN}}^2 |\Psi\rangle \sim |\Psi\rangle. \tag{86}$$

Indeed it is clear that $U_{\mathrm{CN}}^2 \sim U_I$. Moreover, applying U_{CN} twice actually means that we can sequentially apply two physically different transformations which belong to the same equivalence class defined by (85) since the TPS assures that for any pair of logically equivalent operations $U_1 \in U_{\mathrm{CN}}$ and $U_2 \in U_{\mathrm{CN}}$, the overall operation $U_1 U_2$ is equivalent to the weak identity U_I of (81).

The C-NOT gate of (85), together with the Hadamard gate of (26) and phase-shift gate of (27), establish universality [65] for quantum computation with MLE.

7. Multi-qubit operations for MLE

In the case of M qubits, logical equivalence is based on the set of $Z_M = (2^{2M} - 1)$ EA operators

$$\Lambda_r = \lambda_r \otimes \mathbb{1}_{n^M}, \qquad r = \{1, 2, \ldots, Z_M\} \tag{87}$$

where $\mathbb{1}_{n^M}$ is the $n^M \times n^M$ identity matrix and $\{\lambda_r\}$ is the set of $2^M \times 2^M$ matrices which represent the Z_M generators of $\mathrm{SU}(2^M)$. A possible choice of these generators is, for example, the standard Cartan–Weyl basis or its Hermitian variant [66]. The principle of logical equivalence for a pair of multi-qubit states $|\Psi\rangle$ and $|\Psi'\rangle$ will be expressed as usual:

$$|\Psi\rangle \sim |\Psi'\rangle \Leftrightarrow \langle\Psi|\Lambda_r|\Psi\rangle = \langle\Psi'|\Lambda_r|\Psi'\rangle \qquad \text{for all } r. \tag{88}$$

In addition, the states must be normalized.

Unitary logical operations for M qubits, with n-dimensional encoding of every logical basis state, will be elements of the group

$$\mathrm{U}(2^M) \otimes \underbrace{[\mathrm{U}(n) \otimes \cdots \otimes \mathrm{U}(n)]}_{M \text{ times}} \subset \mathrm{U}((2n)^M). \tag{89}$$

Table 3. The group-theoretic structure of unitary logical operations for SLE and MLE of qubits

Encoding	Single qubit	Two qubits	M qubits
$n = 1$	$\mathrm{U}(2)$	$\mathrm{U}(4)$	$\mathrm{U}(2^M)$
$n > 1$	$\mathrm{U}(2) \otimes \mathrm{U}(n)$	$\mathrm{U}(4) \otimes [\mathrm{U}(n) \otimes \mathrm{U}(n)]$	$\mathrm{U}(2^M) \otimes \underbrace{[\mathrm{U}(n) \otimes \cdots \otimes \mathrm{U}(n)]}_{M\text{times}}$

Table 3 summarizes the group-theoretic structure of this mapping from SLE to MLE.

The generalization of the MLE formalism to mixed states and non-unitary logical operations for multiple qubits is straightforward and analogous to the single-qubit case (see section 4).

8. Conclusions

The formalism of MLE of logical basis states presented in this paper is motivated primarily by practical realities such as imperfections and noise in controls, thermally excited initial states, and environmentally induced decoherence.

With MLE, a given logical operation is realized by an infinite number of equivalent physical transformations which may be used interchangeably throughout the computation, thereby allowing for a significant flexibility in the laboratory realizations of control. A crucial point is that MLE naturally suits the application of ultrafast broadband controls which simultaneously drive multiple transitions and have the advantage of generating faster quantum operations, helping to lessen the effect of decoherence.

As presented in section 5 with a simplified model of a single qubit based on Na_2 (which is not efficiently scalable for quantum computing applications in the absence of entanglement), the simulation of closed-loop optimal control of single-qubit MLE operations demonstrates that ultrafast optimal solutions for multilevel systems are readily achievable. Moreover, these solutions are not affected by various decohering processes which are detrimental to quantum information processing based on SLE.

An open question is whether the multiplicity of logically equivalent physical transformations will facilitate the discovery of controls with increased robustness against noise in the control fields. While this assumption is intuitively plausible, a rigorous analysis of the robustness is still required to make any formal conclusions. A powerful method for the robustness analysis is the study of the landscape for optimal control solutions [67]–[69]. Other numerical approaches to the robustness analysis are being considered as well.

An extremely promising feature of MLE is the ability to work with mixed initial states and decoherence without a loss of operational fidelity. If mixing and decoherence are contained within the encoding subspaces, then coherence between the logical basis states will not be affected, meaning that quantum computation with full fidelity is possible. This property, illustrated by a numerical example in section 5, makes MLE a very attractive approach to practical quantum computation.

The TPS of the Hilbert space, which appears in MLE, is a very general feature of multiparticle systems. Therefore, there are many possibilities for building an MLE structure in various physical systems. Interesting examples of systems which could be suitable for MLE are molecules and

trapped ions (with encoding of the logical basis into subspaces of vibrational levels of a molecule or motional sidebands of an ion, respectively). Although we are planning experiments involving diatomic molecules such as Na_2 and K_2 to study the basic functioning of MLE in ultrafast single-qubit operations in the presence of thermalization, we cannot yet specify particular quantum information systems which will benefit most from the use of MLE, since this depends on many technical considerations. Nevertheless, we estimate that the tendency toward faster quantum operations will definitely favour the application of MLE.

Acknowledgments

This work was supported by the NSF, DARPA and NSERC.

Appendix A. Properties of the density matrix components

In (35), we expressed the density matrix of an arbitrary state in the expanded $(2n)$-dimensional Hilbert space as

$$\rho = \sum_{i,j=1}^{2} r_{ij}|i\rangle_{\mathrm{L}\,\mathrm{L}}\langle j| \otimes R_{ij} = \begin{pmatrix} r_{11}R_{11} & r_{12}R_{12} \\ r_{21}R_{21} & r_{22}R_{22} \end{pmatrix}, \tag{A.1}$$

where r_{ij} are matrix elements representing the state of the logical component and R_{ij} are $n \times n$ matrices representing the state of the encoded component. This is a generalization of a pure state, (4):

$$|\psi\rangle = c_0|0\rangle_{\mathrm{L}} \otimes |\boldsymbol{a}\rangle + c_1|1\rangle_{\mathrm{L}} \otimes |\boldsymbol{b}\rangle. \tag{A.2}$$

If the dimension of the encoding subspaces decreases from n to 1, then ρ and $|\psi\rangle$ will represent the logical state of a two-dimensional quantum system:

$$\rho_{\mathrm{L}} = \begin{pmatrix} r_{11} & r_{12} \\ r_{21} & r_{22} \end{pmatrix} \tag{A.3}$$

and

$$|\psi\rangle_{\mathrm{L}} = c_0|0\rangle_{\mathrm{L}} + c_1|1\rangle_{\mathrm{L}}. \tag{A.4}$$

Thus, for encoding subspaces of any dimension, the logical component (ρ_{L} or $|\psi\rangle_{\mathrm{L}}$) represents the state of a two-level qubit. Therefore, ρ_{L} is a proper density matrix, i.e., it is Hermitian, positive and normalized. This normalization means that $\mathrm{Tr}\,(\rho_{\mathrm{L}}) = r_{11} + r_{22} = 1$, where $r_{11},\ r_{22} \geqslant 0$.

In this appendix, we will also show that the matrices R_{11} and R_{22} of the encoded component are proper density matrices that satisfy all necessary properties. The Hermiticity of R_{11} and R_{22} follows directly from the Hermiticity of ρ. Examining the matrix structure of ρ in (A.1), consider the following scenarios:

(i). If $1 \leqslant k, l \leqslant n$, then $\rho_{kl} = (R_{11})_{kl}$, which implies that $(R_{11})_{kl} = (R_{11})^*_{lk}$, meaning $R_{11} = R_{11}^\dagger$.

(ii). If $n+1 \leqslant k, l \leqslant 2n$, then $\rho_{kl} = (R_{22})_{k'l'}$, which implies that $(R_{22})_{k'l'} = (R_{22})^*_{l'k'}$, meaning $R_{22} = R_{22}^\dagger$ (where $k' = k - n$ and $l' = l - n$).

However, if $1 \leqslant k \leqslant n$ and $n+1 \leqslant l \leqslant 2n$, then $\rho_{kl} = (R_{12})_{kl'}$, which implies that $(R_{12})_{kl'} = (R_{21})^*_{k'l}$, meaning $R_{12} = R_{21}^\dagger$.

The positivity of R_{11} and R_{22} also follows directly from the positivity of ρ:

$$\langle\psi|\rho|\psi\rangle \geqslant 0 \text{ for all } |\psi\rangle, \tag{A.5}$$

where

$$\langle\psi|\rho|\psi\rangle = |c_0|^2 r_{11}\langle \boldsymbol{a}|R_{11}|\boldsymbol{a}\rangle + c_0^* c_1 r_{12}\langle \boldsymbol{a}|R_{12}|\boldsymbol{b}\rangle + c_0 c_1^* r_{21}\langle \boldsymbol{b}|R_{21}|\boldsymbol{a}\rangle + |c_1|^2 r_{22}\langle \boldsymbol{b}|R_{22}|\boldsymbol{a}\rangle \geqslant 0. \tag{A.6}$$

In particular, if $|\psi\rangle = |0\rangle_{\mathrm{L}} \otimes |\boldsymbol{a}\rangle$, then $\langle\psi|\rho|\psi\rangle = r_{11}\langle \boldsymbol{a}|R_{11}|\boldsymbol{a}\rangle \geqslant 0$, which implies that $\langle \boldsymbol{a}|R_{11}|\boldsymbol{a}\rangle \geqslant 0$ for any $|\boldsymbol{a}\rangle$. Similarly, if $|\psi\rangle = |1\rangle_{\mathrm{L}} \otimes |\boldsymbol{b}\rangle$, then $\langle \boldsymbol{b}|R_{22}|\boldsymbol{b}\rangle \geqslant 0$ for any $|\boldsymbol{b}\rangle$.

Now consider the normalization condition for the density matrix ρ:

$$\mathrm{Tr}\,(\rho) = r_{11}\mathrm{Tr}(R_{11}) + r_{22}\mathrm{Tr}(R_{22}) = 1. \tag{A.7}$$

Using the normalization of the logical component, $r_{11} + r_{12} = 1$, we obtain

$$r_{11}\mathrm{Tr}(R_{11}) + (1 - r_{11})\mathrm{Tr}(R_{22}) = 1. \tag{A.8}$$

Since the logical and encoding components are independent, i.e., any logical state can be 'attached' to any encoding configuration, (A.8) is satisfied *only* when

$$\mathrm{Tr}(R_{11}) = \mathrm{Tr}(R_{22}) = 1. \tag{A.9}$$

However, note that $\mathrm{Tr}(R_{12}) \neq 1$ and $\mathrm{Tr}(R_{21}) \neq 1$ in general.

In conclusion, this appendix demonstrates that the density matrix components ρ_{L}, R_{11} and R_{22} are Hermitian, positive and normalized (of unit trace), and therefore are proper density matrices.

References

[1] Nielsen M A and Chuang I L 2000 *Quantum Computation and Quantum Information* (Cambridge: Cambridge University Press)
[2] Quantum Information Science and Technology Roadmapping Project http://qist.lanl.gov
[3] van Enk S J and Kimble H J 2001 *Quantum Inform. Comput.* **2** 1
[4] Shor P W 1996 *Proc. 37th Annu. Symp. on the Foundations of Computer Science* (Los Alamitos, CA: IEEE Computer Society Press)
[5] Rabitz H, de Vivie-Riedle R, Motzkus M and Kompa K 2000 *Science* **288** 824
[6] Rabitz H and Walmsley I 2003 *Phys. Today* **56** 43
[7] Judson R S and Rabitz H 1992 *Phys. Rev. Lett.* **68** 1500
[8] Zhang H and Rabitz H 1994 *Phys. Rev.* A **49** 2241
[9] Demiralp M and Rabitz H 1998 *Phys. Rev.* A **57** 2420
[10] Geremia J M, Zhu W and Rabitz H 2000 *J. Chem. Phys.* **113** 10841
[11] Turinici G and Rabitz H 2001 *Chem. Phys.* **267** 1

[12] Hornung T, Motzkus M and de Vivie-Riedle R 2002 *Phys. Rev.* A **65** 021403
[13] Ramakrishna V and Rabitz H 1996 *Phys. Rev.* A **54** 1715
[14] Sanders G D, Kim K W and Holton W C 1999 *Phys. Rev.* A **59** 1098
[15] Brif C, Rabitz H, Wallentowitz S and Walmsley I A 2001 *Phys. Rev.* A **63** 063404
[16] Tesch C M, Kurtz L and de Vivie-Riedle R 2001 *Chem. Phys. Lett.* **343** 633
[17] Tesch C M and de Vivie-Riedle R 2002 *Phys. Rev. Lett.* **89** 157901
[18] Troppmann U, Tesch C M and de Vivie-Riedle R 2003 *Chem. Phys. Lett.* **378** 273
[19] Palao J P and Kosloff R 2002 *Phys. Rev. Lett.* **89** 188301
[20] Amitay Z, Kosloff R and Leone S R 2002 *Chem. Phys. Lett.* **359** 8
[21] Vala J, Amitay Z, Zhang B, Leone S R and Kosloff R 2002 *Phys. Rev.* A **66** 062316
[22] Sklarz S E and Tannor D J 2004 Local control theory for unitary transformations: application to quantum computing without leakage *Preprint* quant-ph/0404081
[23] Zadoyan R, Kohen D, Lidar D A and Apkarian V A 2001 *Chem. Phys.* **266** 323
[24] Bihary Z, Glenn D R, Lidar D A and Apkarian V A 2002 *Chem. Phys. Lett.* **360** 459
[25] Walmsley I and Waxer L 1998 *J. Phys. B: At. Mol. Opt. Phys.* **31** 1825
[26] Weiner A M 2000 *Rev. Sci. Instrum.* **71** 1929
[27] Brixner T, Damrauer N H and Gerber G 2001 *Adv. Atom. Mol. Opt. Phys.* **46** 1
[28] Brixner T, Damrauer N H, Krampert G, Niklaus P and Gerber G 2003 *J. Mod. Opt.* **50** 539
[29] Levis R J, Menkir G M and Rabitz H 2001 *Science* **292** 709
[30] Levis R J and Rabitz H A 2002 *J. Phys. Chem.* A **106** 6427
[31] Dudovich N, Oron D and Silberberg Y 2002 *Nature* **418** 512
[32] Oron D, Dudovich N and Silberberg Y 2003 *Phys. Rev. Lett.* **90** 213902
[33] Cirac J I and Zoller P 1995 *Phys. Rev. Lett.* **74** 4091
[34] Poyatos J F, Cirac J I and Zoller P 1998 *Phys. Rev. Lett.* **81** 1322
[35] Sørensen A and Mølmer K 1999 *Phys. Rev. Lett.* **82** 1971
Sørensen A and Mølmer K 2000 *Phys. Rev.* A **62** 022311
[36] Jonathan D, Plenio M B and Knight P L 2000 *Phys. Rev.* A **62** 042307
[37] Milburn G J, Schneider S and James D F V 2000 *Fortschr. Phys.* **48** 801
[38] Wineland D J, Monroe C, Itano W M, Leibfried D, King B E and Meekhof D M 1998 *J. Res. Natl. Inst. Stand. Technol.* **103** 259
[39] Leibfried D, Blatt R, Monroe C and Wineland D 2003 *Rev. Mod. Phys.***75** 281
[40] García-Ripoll J J, Zoller P and Cirac J I 2003 *Phys. Rev. Lett.* **91** 157901
[41] Bartelt A, Roth M, Mehendale M and Rabitz H 2005 *Phys. Rev.* A **71** 063806
[42] Zanardi P, Lidar D A and Lloyd S 2004 *Phys. Rev. Lett.* **92** 060402
[43] Knill E and Laflamme R 1997 *Phys. Rev.* A **55** 900
[44] Kribs D, Laflamme R and Poulin D 2005 *Phys. Rev. Lett.* **94** 180501
[45] Huber K P and Herzberg G 1970 *Molecular Spectra and Molecular Structure: IV. Constants of Diatomic Molecules* (New York: Van Nostrand Reinhold)
[46] Ahn J, Weinacht T C and Bucksbaum P H 2000 *Science* **287** 463
[47] Ahn J, Rangan C, Hutchinson D N and Bucksbaum P H 2002 *Phys. Rev.* A **66** 022312
Rangan C, Ahn J, Hutchinson D N and Bucksbaum P H 2002 *J. Mod. Opt.* **49** 2339
[48] Cerf N J, Adami C and Kwiat P G 1998 *Phys. Rev.* A **57** R1477
[49] Kwiat P G, Mitchell J R, Schwindt P D D and White A G 2000 *J. Mod. Opt.* **47** 257
[50] Londero P, Dorrer C, Anderson M, Wallentowitz S, Banaszek K and Walmsley I A 2004 *Phys. Rev.* A **69** 010302
[51] Lloyd S 2000 *Phys. Rev.* A **61** 010301
[52] Meyer D A 2000 *Phys. Rev. Lett.* **85** 2014
[53] Brennen G K, Caves C M, Jessen P S and Deutsch I H 1999 *Phys. Rev. Lett.* **82** 1060

[54] Brennen G K, Deutsch I H and Jessen P S 2000 *Phys. Rev.* A **61** 062309
Deutsch I H, Brennen G K and Jessen P S 2000 *Fortschr. Phys.* **48** 925
[55] Brennen G K, Deutsch I H and Williams C J 2002 *Phys. Rev.* A **65** 022313
[56] Jaksch D, Briegel H -J, Cirac J I, Gardiner C W and Zoller P 1999 *Phys. Rev. Lett.* **82** 1975
[57] Calarco T, Hinds E A, Jaksch D, Schmiedmayer J, Cirac J I and Zoller P 2000 *Phys. Rev.* A **61** 022304
[58] Calarco T, Dorner U, Julienne P S, Williams C J and Zoller P 2004 *Phys. Rev.* A **70** 012306
[59] DeMille D 2002 *Phys. Rev. Lett.* **88** 067901
[60] Vager D, Segev B and Band Y B 2005 *Phys. Rev.* A **72** 022325
[61] Saffman M and Walker T G 2005 *Phys. Rev.* A **72** 022347
Saffman M and Walker T G 2005 *Phys. Rev.* A **72** 042302
[62] Lee C and Ostrovskaya E A 2005 *Phys. Rev.* A **72** 062321
[63] Dunn T J, Sweetser J N, Walmsley I A and Radzewicz C 1993 *Phys. Rev. Lett.* **70** 3388
[64] Branderhorst M P A, Londero P, Wasylczyk P, Walmsley I A, Brif C, Rabitz H and Kosut R L 2006 Coherent control of decoherence in diatomic molecules (unpublished)
[65] DiVincenzo D P 1995 *Phys. Rev.* A **51** 1015
[66] Barut A O and Raczka R 1987 *Theory of Group Representations and Applications* 2nd edn (Singapore: World Scientific) ch 1
[67] Rabitz H A, Hsieh M M and Rosenthal C M 2004 *Science* **303** 1998
[68] Rabitz H, Hsieh M and Rosenthal C 2005 *Phys. Rev.* A **72** 052337
[69] Brif C, Rabitz H, Hsieh M, Walmsley I and Kosut R 2006 Robustness of optimally controlled unitary quantum operations (unpublished)